

Aerodynamic Jump Simulation Analysis and Trajectory Deflections for Projectiles Launched at Supersonic Speeds

Dimitrios N. Gkritzapis¹ and George Kaimakamis²

Abstract

The present study investigates the aerodynamic jump phenomenon effects on flat-fire no-wind unguided flight trajectory disturbances for projectiles designed to be launched at supersonic speeds in forward fire from air vehicles. The ammunition used is the 30 mm diameter XM788 projectile firing from M230 machine automatic cannon. The modified linear flight simulation model is applied for the free-flight atmospheric motion prediction of the examined projectile including the variable behavior of the most significant aerodynamic forces and moments coefficients, which have been taken from official tabulated database.

Mathematics Subject Classification: 70B10

¹ Department of Mathematical and Engineering Sciences, Hellenic Military Academy, Vari, Attiki, 16673, Greece, e-mail: gritzap@yahoo.gr

² Department of Mathematical and Engineering Sciences, Hellenic Military Academy, Vari, Attiki, 16673, Greece, e-mail: gmiamis@gmail.com

Keywords: Aerodynamic Jump Phenomenon; 30 mm XM788 projectile; Modified Linear Trajectory Simulation; Supersonic Firing; Trajectory Deflection

1 Introduction

The importance of the aerodynamic jump phenomena on the trajectories of flat-fire spinning projectiles is sufficient for the precision of firing sidewise from air vehicles. However, for high-velocity, small yaw, flat-fire atmospheric motions, these effects are often much larger than the drift, at moderate ranges.

The trajectory deflections caused by aerodynamic jump on a .30 caliber machine gun bullet was first addressed in 1943 [1]. Various authors have simulated the aerodynamic jump phenomenon caused by aerodynamic asymmetry, lateral force impulses, and non-linear forces and moments [2, 3, 4].

A modified linear flight dynamic model with variable aerodynamic coefficients is applied for rapid trajectory prediction [5]. The computational results of the above trajectory model have already verified compared to the corresponding full 6-DOF simulations for the 105 mm diameter spin-stabilized projectile, the 120 mm diameter fin-stabilized projectile and the 7.62 mm diameter small bullet [6, 7].

In the present paper, the above flight simulation model is applied for the no-wind unguided atmospheric trajectory motions and flat-fire launched disturbances due to aerodynamic jump performance for projectiles firing at supersonic speeds with different angles relative to the air vehicle's flight path motion.

2 Projectile Model

The present analysis considers a type of 30 mm cartridge [8]. The XM788 target practice (TP) has a blue painted projectile with white markings. The inert/solid projectile is a three piece assembly consisting of steel body with cavity, rotating band and aluminum nose piece. Furthermore, the cartridge case is aluminum.

Basic physical and geometrical characteristics data of the above-mentioned 30 mm XM788 cartridge type are illustrated briefly in Table 1. This projectile is fired from M230 machine automatic cannon placed on ground surface or low-speed helicopters, as illustrated in Figure 1.

Table 1: Physical and geometrical data of the examined projectile type

Characteristics	30 mm XM788 cartridge
Reference diameter D , mm	29.92
Total length L , mm	199.77
Total mass m , gr	329
Axial moment of inertia I_{XX} , $\text{kg}\cdot\text{m}^2$	$3.302\cdot 10^{-5}$
Transverse moment of inertia I_{YY} , $\text{kg}\cdot\text{m}^2$	$1.743\cdot 10^{-4}$



Figure 1: M230 machine automatic gun.

3 Modified Linear Flight Simulation Model

The projectile can be modelled as a rigid body possessing six degrees-of-freedom (6-DOF) including three inertial position components of the system mass center as well as the three Euler orientation angles. Two mean coordinate systems are used for the computational analysis of the atmospheric flight trajectory path. The one is a plane fixed (inertial frame), at the ground surface, which its center lies on the projection of the firing point on ground surface. The other is a no-roll rotating coordinate system that is attached to, and moving with, the projectile's center of mass (no-roll-frame).

The twelve state variables x , y , z , φ , θ , ψ , \tilde{u} , \tilde{v} , \tilde{w} , \tilde{p} , \tilde{q} and \tilde{r} are necessary to describe position, flight direction and velocity at every point of the projectile's atmospheric trajectory path. Introducing the components of the acting forces and moments expressed in the no-roll-frame (\sim) with the dimensionless arc length l measured in calibers of travel, as an independent variable, the following equations of motion are derived:

$$\frac{dx}{dl} = \frac{D}{V_T} \cos \psi \cos \theta \tilde{u} - \frac{D}{V_T} \sin \psi \tilde{v} + \frac{D}{V_T} \cos \psi \sin \theta \tilde{w} \quad (1)$$

$$\frac{dy}{dl} = \frac{D}{V_T} \cos \theta \sin \psi \tilde{u} + \frac{D}{V_T} \cos \psi \tilde{v} + \frac{D}{V_T} \sin \psi \sin \theta \tilde{w} \quad (2)$$

$$\frac{dz}{dl} = -\frac{D}{V_T} \sin \theta \tilde{u} + \frac{D}{V_T} \cos \theta \tilde{w} \quad (3)$$

$$\frac{d\varphi}{dl} = \frac{D}{V_T} \tilde{p} + \frac{D}{V_T} \tan \theta \tilde{r} \quad (4)$$

$$\frac{d\theta}{dl} = \frac{D}{V_T} \tilde{q} \quad (5)$$

$$\frac{d\psi}{dl} = \frac{D}{V_T \cos \theta} \tilde{r} \quad (6)$$

$$\frac{d\tilde{u}}{dl} = -\frac{D}{V_T} g \sin \theta - F_1 V_T C_D + \frac{D}{V_T} \tilde{v} \tilde{r} - \frac{D}{V_T} \tilde{q} \tilde{w} \quad (7)$$

$$\frac{d\tilde{v}}{dl} = -F_1 (C_{LA} + C_D) \tilde{v} - \frac{D}{V_T} \tilde{r} \tilde{w} \tan \theta - \frac{D}{V_T} \tilde{u} \tilde{r} \quad (8)$$

$$\frac{d\tilde{w}}{dl} = \frac{D}{V_T} g \cos \theta - F_1 (C_{LA} + C_D) \tilde{w} + \frac{D}{V_T} \tilde{u} \tilde{q} + \tan \theta \frac{D}{V_T} \tilde{r} \tilde{v} \quad (9)$$

$$\frac{d\tilde{p}}{dl} = \frac{\pi \rho D^5}{16 I_{XX}} C_{LP} \tilde{p} \quad (10)$$

$$\begin{aligned} \frac{d\tilde{q}}{dl} = & 2 F_2 (C_{LA} + C_D) L_{CGCP} \tilde{w} + \frac{D}{V_T} F_2 C_{MPA} L_{CGCM} \tilde{p} \tilde{v} + \\ & + D^2 F_2 C_{MQ} \tilde{q} + 2 D F_2 C_{MA} - \frac{D}{V_T} \frac{I_{XX}}{I_{YY}} \tilde{p} \tilde{r} - \frac{D}{V_T} \tan \theta \tilde{r}^2 \end{aligned} \quad (11)$$

$$\begin{aligned} \frac{d\tilde{r}}{dl} = & -2 F_2 (C_{LA} + C_D) L_{CGCP} \tilde{v} + \frac{D}{V_T} F_2 C_{MPA} L_{CGCM} \tilde{p} \tilde{w} + \\ & + D^2 F_2 C_{MQ} \tilde{r} - 2 D F_2 C_{MA} + \frac{D}{V_T} \frac{I_{XX}}{I_{YY}} \tilde{p} \tilde{q} + \frac{D}{V_T} \tan \theta \tilde{q} \tilde{r} \end{aligned} \quad (12)$$

where $F_1 = \pi \rho D^3 / 8m$, $F_2 = \pi \rho D^3 / 16 I_{YY}$ are dimensional coefficients, L_{CGCM} is the distance from the center of gravity (CG) to the Magnus center of pressure (CM) along the station line, and L_{CGCP} is the distance from the center of gravity (CG) to the aerodynamic center of pressure (CP) along the station line.

In these equations various simplifications were employed such as: (i) small yaw angle ψ , (ii) aerodynamic angles of attack α and sideslip β remain small ($< 15^\circ$) for the main part of the trajectory, (iii) Magnus force components are small in comparison with the weight and aerodynamic force components, and so they are treated as negligible, and (iv) projectile is geometrically and aerodynamically symmetric about the station line.

The above twelve first order ordinary differential equations are solved simultaneously by resorting to numerical integration using a 4th order

Runge-Kutta method. The aerodynamic coefficients C_D , C_{LA} , C_{MPA} , C_{MQ} , C_{MA} are projectile-specific functions of the Mach number and total angle of attack variations for the examined 30mm XM788 projectile type [8]. On the other hand, the roll damping aerodynamic coefficient C_{LP} is not varying important with Mach number taking the constant mean value $C_{LP} = -0.015$ for the main part of the projectile firing-to-target trajectory path.

4 Atmospheric Simulation Model

Atmospheric properties of air, like density ρ , are being calculated based on a standard atmosphere from the International Civil Aviation Organization (ICAO).

5 Aerodynamic Jump Simulation Analysis

For modern high-velocity, small yaw, flat-fire atmospheric trajectories the aerodynamic jump phenomenon [9, 10] is simulated by the following expression:

$$J_A = -K_X^2 \left(\frac{C_{LA}}{C_{MA}} \right) \left(\frac{2\pi}{\eta} \right) \sin \beta_o \quad (13)$$

where K_X^2 is the non-dimension axial moment of inertia, C_{LA} and C_{MA} are lift and overturning moment aerodynamic coefficients of the 30mm diameter XM788 projectile at the firing point, η is the rifling right-hand twist rate of the M230 machine gun with helix angle of $6^\circ 30'$ (27.6 calibers/turn), and β_o is the pure sideslip (yaw) angle (zero pitch component), as illustrated in Figure 2, expressed in the form:

$$\sin \beta_o = \left(\frac{V_{hel}}{V_o} \right) \sin \omega \quad (14)$$

Firing sidewise with V_{fir} at an angle ω relative to the helicopters flight path motion V_{hel} (Figure 2), the total initial muzzle velocity of the projectile V_o is

$$V_o = \sqrt{V_{fir}^2 + V_{hel}^2 + 2 V_{fir} V_{hel} \cos \omega} \quad (15)$$

Equation (14) combining with equation (13) gives the following engineering correlation formula for the aerodynamic jump performance for flat-firing sidewise from air vehicles:

$$J_A = -K_X^2 \left(\frac{C_{LA}}{C_{MA}} \right) \left(\frac{2\pi}{\eta} \right) \left(\frac{V_{hel}}{V_o} \right) \sin \omega \quad (16)$$

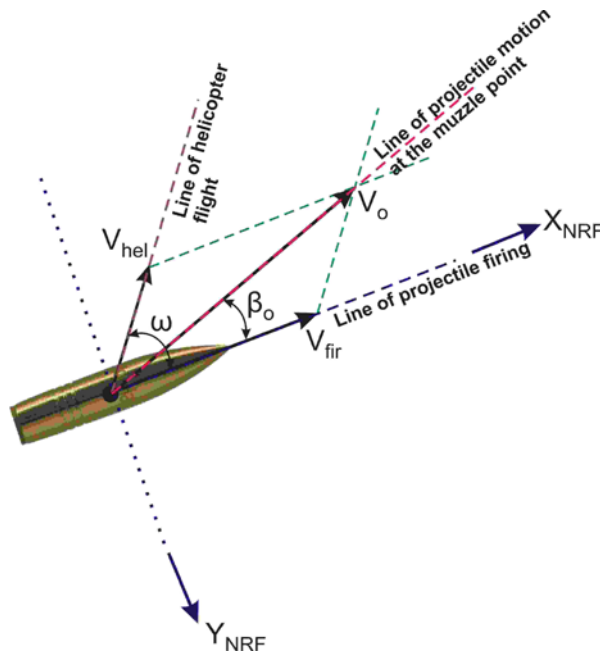


Figure 2: Top view of the initial muzzle velocity at the firing point from M230 helicopter automatic cannon.

The vertical deflection D_Z to target impact point produced by the aerodynamic jump performance due to initial flat-firing sidewise is:

$$D_Z = (J_A) \cdot (Range) \quad (17)$$

6 Computational Results

The present computational analysis deals with the 6-DOF no-wind unguided flat-fire atmospheric trajectory motion of the 30mm diameter XM788 projectile type, using the modified linear flight dynamic model with variable aerodynamic and Magnus coefficients. Horizontal fire is assumed firing at three different angles ω (10, 20 and 30 deg) with α 805 m/s supersonic velocity relative to the helicopter's low speed of 100 knots (almost 50 m/s).

The target impact point predictions firing at 300 m height, as shown in the additional zoomed picture in Figure 3a, are 2,797 m, 2,794 m and 2,789 m at angles 10, 20 and 30 deg, respectively. Few meters difference in the final target shooting area is significant for a small projectile like 30mm diameter XM788.

On the other hand, firing sidewise at 100 m height, the corresponding target impact points are 1,997m, 1,994m and 1,989m at the same angles ω relative to helicopter's flight path direction, as illustrated in better form in the additional zoomed picture in Figure 3b.

The total flight time firing from 300 m height at 30 deg, relative to helicopter's automatic machine gun velocity, is almost 9.5 s. The corresponding value for flat-launching at 100 m height is at about 5.3 s. The above results state that, the time of projectile flight motion is short so the applied variable rapid trajectory prediction must be taken into account for high accuracy impact target shooting.

The vertical deflections to target shooting area caused by the aerodynamic jump performance firing from 300 m height above mean sea level at firing angles $\omega \pm 10$ deg, ± 30 deg and ± 50 deg, respectively, at the first 200 m range, are illustrated in Figure 4.

The computational simulation gives -9.3 cm, -28 cm and -41 cm vertical deflections corresponding to 2m, 6m and 9m horizontal deflections for positive firing angles 10, 30 and 50 degrees, respectively. For negative firing angles ω the projectile strikes the target with positive vertical deflections.

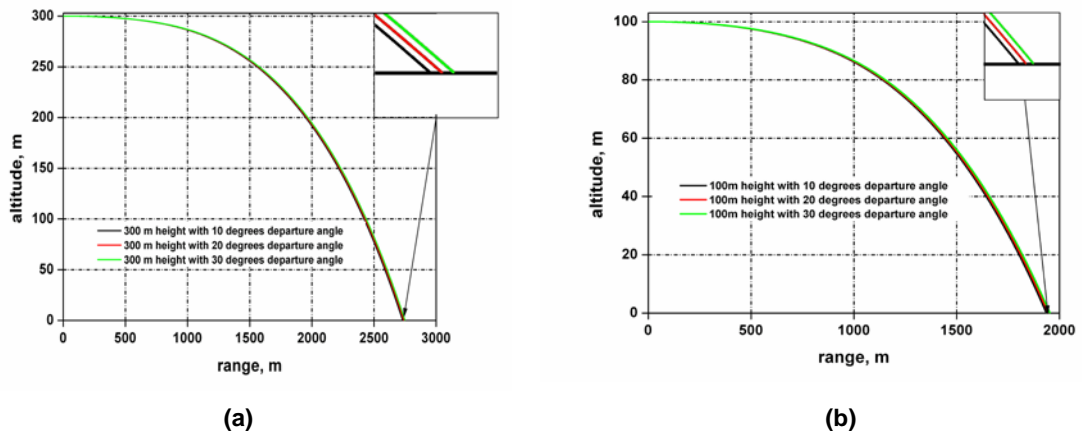


Figure 3: Atmospheric trajectory simulations firing sideways relative to helicopter's flight path motion at 300 m and 100 m heights.

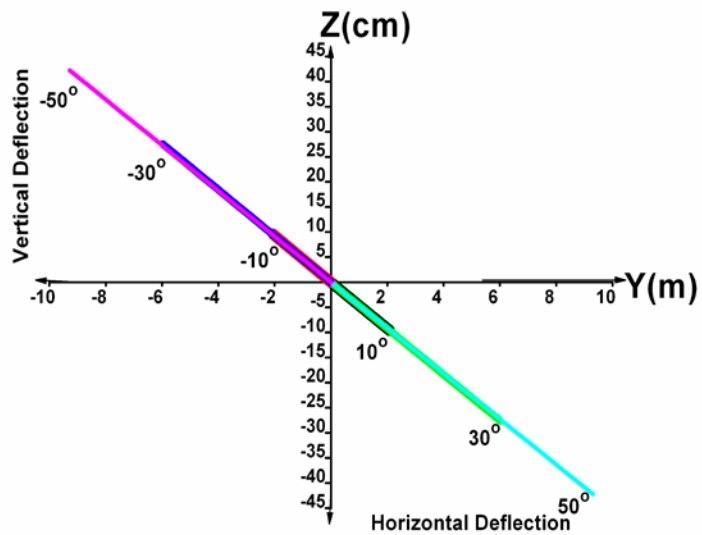


Figure 4: Vertical deflections produced by aerodynamic jump phenomenon firing at positive and negative launching angles from 300 m height.

7 Conclusion

The modified linear flight simulation model with variable aerodynamic force and moment coefficients based on Mach number variations and total angle of attack effects is applied for the atmospheric trajectory simulations of the 30 mm diameter XM788 projectile firing sidewise from low-speed helicopter.

A simple engineering correlation formula based on the physical, geometric and aerodynamic characteristics of the projectile, the initial muzzle firing velocity and the air vehicle's flight speed is applied for the flat-fire trajectory deflections due to aerodynamic jump performance.

References

- [1] T.H. Sterne, *On Jump due to Bore Clearance*, Ballistic Research Laboratories, Report No. **491**, (1944).
- [2] G. Cooper, *Extending the Jump Analysis for Aerodynamic Asymmetry*, Army Research Laboratory, ARL-TR-**3265**, (2004), 1-4.
- [3] B. Burchett, A. Peterson and M. Costello, Prediction of Swerving Motion of a Dual-Spin Projectile with Lateral Pulse Jets in Atmospheric Flight, *Mathematical and Computer Modeling*, **35**(1-2), (2002), 1-14.
- [4] R.L. McCoy, *Modern Exterior Ballistics*, Schiffer, Attlen, PA, 1999.
- [5] L. Hainz and M. Costello, Modified Projectile Linear Theory for Rapid Trajectory Prediction, *Journal of Guidance, Control, and Dynamics*, **28**(5), (2005), 1007-1009.
- [6] D.N. Gkritzapis, D.P. Margaris, E.E. Panagiotopoulos, G. Kaimakamis and K. Siassiakos, Prediction of the Impact Point for Spin and Fin Stabilized Projectiles, *WSEAS Transactions on Information Science and Applications*, **5**(12), (2008), 1667-1676.

- [7] D.N. Gkritzapis, E.E. Panagiotopoulos, D.P. Margaritis and D.G. Papanikas, Computational Atmospheric Trajectory Simulation Analysis of Spin-Stabilized Projectiles and Small Bullets, *International Journal of Computing Science and Mathematics*, **2**(1/2), (2008), 53-72.
- [8] R.L. McCoy, *Aerodynamic characteristics of the 30mm XM788 and XM789 projectiles*, Ballistic Research Laboratories, Report No. **2432**, (1982).
- [9] D.N. Gkritzapis, E.E. Panagiotopoulos, D.P. Margaritis and D.G. Papanikas, Flat-Fire Aerodynamic Jump Performance of Projectiles Fired from a Helicopter, *Journal of Battlefield Technology*, **11**(2), (2008), 1-8.
- [10] D.N. Gkritzapis, E.E. Panagiotopoulos, In-Bore Yaw Effects on Lateral Throw-off and Aerodynamic Jump Behavior for Small Caliber Projectiles Firing Sidewise from Air Vehicles, *Journal of Applied Mechanics*, **78**(5), (2011), 051017-1 up to 051017-7.